ELSEVIER

Polymer 42 (2001) 4619–4633

polymer

www.elsevier.nl/locate/polymer

Structure–property relationships of poly(tetrafluoroethylene)–poly(tetrafluoroethylene-*co*-vinylidene fluoride-*co*-hexafluoropropylene) blends

B.D. Kaushiva[a], G.L. Wilkes[a,*], C. Comeaux[b], L. Socha[b]

[a]*Polymer Materials and Interfaces Laboratory, Department of Chemical Engineering, Virginia Polytechnic Institute and State University, Blacksburg, VA 24061-0211, USA*

[b]*Chemfab Corp., Merrimack, NH 03054-1137, USA*

Received 26 June 2000; received in revised form 8 November 2000; accepted 8 November 2000

Abstract

The morphology and mechanical properties of emulsion blended samples of poly(tetrafluoroethylene) (PTFE) and poly(tetrafluoroethylene-*co*-vinylidene fluoride-*co*-hexafluoropropylene) (FKM) were investigated. Film samples with varying levels of PTFE content and varying degrees of FKM covalent cross-linking were produced. It was observed at room temperature that below 50 wt% PTFE content, cross-linking the FKM can have a much larger influence on the tensile modulus than changing the PTFE content. Above 50 wt% PTFE, however, the modulus showed a near exponential increase with respect to increasing PTFE content. Without cross-linking, the toughness of the cast blends was shown to systematically decrease as the PTFE content was increased. However, when the FKM was cross-linked in film-form with 20–60 wt% PTFE, more stress was apparently transferred to the PTFE particulate leading to a higher elongation-to-break and a higher toughness. DMA analyses revealed a systematic increase of the storage moduli with increasing PTFE content. A tan δ peak at ca. -10°C was observed which corresponds to the glass transition of the FKM and the magnitude of this peak was observed to decrease systematically with decreasing FKM content or with increasing levels of FKM cross-linking. For the levels of cross-linking tested, however, this peak reduction due to cross-linking was not observed to be as significant as increasing the PTFE content. For all PTFE content levels studied, the transmission electron microscopy (TEM) examination revealed a dispersed morphology for the PTFE particulate with the FKM forming a continuous matrix. The PTFE particulate were observed to be ca. 0.2 μm in size and only slightly aggregated. The phase images from the tapping-mode atomic force microscopy showed that this is a useful technique for imaging morphology that lies parallel to the plane of the film surface, and for developing correlations with the TEM results of the bulk structure.

Keywords: Fluoropolymer; Poly(tetrafluoroethylene); Fluoroelastomer

1. Introduction

The unusually high thermal stability, the environmental resistance, and the chemical inertness of fluoropolymers is well known, and makes the use of these materials desirable for many demanding applications [1]. However, matching the mechanical properties to the required performance specifications has presented many challenges. For example, poly(tetrafluoroethylene) (PTFE) and other fluoroplastics have high moduli but are also prone to creep and are generally difficult to process [2,3]. Fluoroelastomers are ideal under extreme conditions where the polymer must bear much deformation and absorb considerable mechanical energy, but they must be cross-linked to reduce creep and improve modulus. Reducing the glass transition temperature of the fluoroelastomers and improving the stability of their cross-links have been the subject of much research since the 1940s [3]. Rather than adding a common filler such as carbon black [4], blending a fluoroplastic with a fluoroelastomer presents the opportunity to exploit the desirable properties of each. This research will thus seek to examine the utility of using PTFE to reinforce a fluoroelastomeric matrix. Fluoroelastomers are commonly produced by copolymerizing the various fluoromonomers which are available, and so this research used the terpolymer of the random copolymerization of tetrafluoroethylene, vinylidene fluoride, and hexafluoropropylene-—- poly(tetrafluoroethylene-*co*-vinylidene fluoride-*co*-hexafluoropropylene) (FKM) [3].

* Corresponding author. Tel.: +1-540-231-5498; fax: +1-540-231-9511.
E-mail address: gwilkes@vt.edu (G.L. Wilkes).

0032-3861/01/$ - see front matter
PII: S0032-3861(00)00832-6

The unique structure of PTFE gives this polymer many unusual and useful characteristics. The high stability of the carbon–fluorine bonds makes it chemically inert even at high temperatures and the bulkiness of the pendant fluorine atoms, relative to hydrogen, provides an additional shielding effect for the carbon backbone of the molecule. PTFE also exhibits unusual toughness at temperatures as low as −273°C, yet it possesses a remarkably high nascent crystalline melt temperature of 342°C [1]. High molecular weight PTFE (ca. 10^6–10^7 Da) has a very high melt viscosity of ca. 10^{11} poise at 380°C [1,2]. Its outstanding thermal stability provides this polymer with useful properties over a 550°C range [1] PTFE also has a very low dielectric constant (ca. 2.1) and dissipation factor (<0.0004) that are both stable over a broad range of temperatures and frequencies (60–10^9 Hz) [1]. The combination of these properties together with its well-known low friction coefficient, excellent weatherability, and low surface free energy allow PTFE to perform well in many demanding environments, making it an ideal polymer uniquely suited for a variety of specialty applications [3]. Some of these applications include surface coatings, casting films, architectural fabrics, acoustic membranes, expansion joint materials, flexible braided hose, conveyor belts, gaskets, electrical insulation, and fire-resistant thermal insulation [1,5].

On the other hand, PTFE does have some properties which require special techniques to be applied for its analysis and application. It is insoluble in all common solvents below 300°C, limiting characterization by typical methods such as gel permeation chromatography, osmometry, or other common solution characterization methods [6]. Therefore, the PTFE molecular weight is usually classified by melt viscosity at 380°C or through correlations based on specific gravity or percent crystallinity [2,6]. Its very high melt viscosity generally precludes the use of conventional polymer processing techniques such as injection molding or melt extrusion [1]. Lower molecular weight PTFE (melt viscosity below ca. 10^9 poise at 380°C) is brittle but, because it retains its low coefficient of friction, it is often applied as a dry lubricant [6]. Greater toughness is obtained at molecular weights of ca. 10^6–10^7 Da (10^{10}–10^{12} poise at 380°C); however, once the high molecular weight PTFE has been melted, regaining its high nascent crystallinity is not possible due to molecular constraints such as enhanced chain entanglement [2,6]. Because of these considerations, the most commonly utilized processing techniques all incorporate a 'sintering' step after molding and pressing the granular resins into the desired shape followed by heating above the melt temperature [2]. The cooling rate can be controlled to achieve the desired level of crystallinity (although below the nascent crystalline fraction) after the heat treatment and this new percent crystallinity largely determines the final mechanical properties of the polymer [1]. The other major type of operation used involves spinning fibers or coating materials using aqueous dispersions of PTFE and these methods frequently also include a sintering step [1].

PTFE is generally produced via a free radical polymerization typically performed under moderate pressure (100–1000 psi) and in warm water (ca. 60–95°C) [3]. The most common initiator used for this polymerization is a mixture of potassium persulfate, hydrogen peroxide, and oxygen [3,7]. Abstraction reactions are not thermodynamically favorable for fluorocarbons, thus there is minimal chain transfer or disproportionation [3]. Termination therefore occurs by combination, principally resulting in one PTFE molecule for each persulfate ion decomposed [3]. Two techniques are generally employed for the polymerization of PTFE. Suspension polymerization in an aqueous medium utilizes vigorous agitation and little or no dispersing agent [2]. The product from this method precipitates into granular resins which are produced in a wide variety of grades tailored to meet the desired flow specifications and end-use properties [2]. These granular resins are typically composed of high molecular weight, ca. 1 mm sized particles which have very high nascent crystallinity (ca. 95% or higher) [3]. Emulsion polymerization is the other main technique and it is also called 'aqueous dispersion polymerization'. This process utilizes mild agitation and adequate amounts of dispersing agents (such as perfluorocarboxylic acid) to yield a very different product [2,3]. Although still of high molecular weight and high nascent crystallinity, the product of this technique is a stable dispersion of small, colloidal particles ca. 0.2–0.3 μm in size [6]. Whereas the granular resin products can be molded into various shapes by pressing and sintering, the aqueous dispersions are generally used for dispersion coating or paste extrusion [2].

It should be emphasized that both these polymerization techniques are generally used to yield high molecular weight polymer. One substantial difference between the high and low molecular weight polymers is that the nascent particles of high molecular weight PTFE readily fibrillate under shear [6,8]. The extended chain crystalline morphology develops easily from the nascent structure because the PTFE molecule is not highly branched and because the rapid crystallization during polymerization precludes the formation of many entanglements. This fibrillation can lead to the formation of a physical network of fibers which rapidly becomes unworkable [6]. Low molecular weight particles do elongate to some extent, but then disintegrate, as stated earlier, into the powder form that is useful as a dry lubricant [2,6]. The ease with which high molecular weight PTFE fibrillates, leading to dramatic changes in its properties, substantially limits the usefulness of this material, particularly where much mechanical work will be borne by the polymer. On the other hand, many applications would greatly benefit from its unique combination of properties, if it could be incorporated. This challenge has led to the development of a new class of materials which are

Table 1
General formulation for the fluoroelastomer/fluoroplastic blends

	Parts dry weight by dry weight of rubber
FKM	100
PTFE	Varied
Zinc oxide	10
Diak #3	5
Daxad 11 solution	1.5
Ammonium caseinate	1.5

based on reinforcing a fluoroelastomeric matrix with a high molecular weight fluoroplastic particulate [9]. The problems associated with blending PTFE have meant that earlier applications of this concept used milling to press the PTFE microparticulate into the fluorinated elastomer which was subsequently cross-linked [6]. This milling process required micropowders of low molecular weight PTFE to be used in order to avoid the processing problems associated with fibrillation [6]. Also, such additions by milling were limited to ca. 25 wt% PTFE [6].

In this work we utilize the product of emulsion polymerization. This processing technique blends aqueous dispersions of high molecular weight PTFE, fluoroelastomeric latexes, and curative agents [6,9,10]. These blends are then cast on to a carrier film and dried as described in Refs. [6,11]. The materials are then thermally cured, which promotes the cross-linking reactions in the elastomer [6]. This yields a very flexible product which can be produced with homogeneously dispersed filler particles of up to 70 wt% PTFE [6]. Moreover, the use of high molecular weight PTFE provides the possibility later of inducing fibrillation and providing additional reinforcement [6].

Several factors can be varied in these systems to produce the desired properties. The PTFE content in the formulation can be adjusted to obtain higher modulus while other fillers may also be added to the system. Different plastic and elastomeric components could also be used. To some extent, the degree of cross-linking can be controlled and the mechanism used for cross-linking could also be changed to improve the stability of the cross-links. Furthermore, the possibility of fibrillating the PTFE component suggests another possible way to increase the modulus at a given PTFE content and degree of cross-linking. For example, fibrillation could possibly be induced by applying shear to the film surface, thus altering the surface properties relative to the matrix. Given all of these various ways to control the properties of these new materials, it can be seen that a better understanding of how the variables relate to the final properties would be of great importance in further optimizing the mechanical performance of these systems. Therefore, this research sought to focus on some compositions of industrial importance and explored the structure–property behavior based on two variables: the ratio of PTFE to fluoroelastomer and the degree of FKM cross-linking.

2. Experimental

2.1. Materials

The materials used in this study were produced by blending the components while still in an emulsified, microparticulate form. Particle sizes for the polymeric components generally ranged from 0.01 to 1.0 μm. In the components for this study, the average particle size in the aqueous state was determined to be 0.2 μm using a Leeds & Northrup Microtrac ultrafine particle size analyzer, which measures size via dynamic light scattering. Prior to blending with the other components in the formulations described later in this section, the aqueous latexes of fluoroelastomer were concentrated to facilitate the casting process using standard industrial creaming techniques [6].

Vertical casting of the blend utilized a carrier film [11] which was pulled through the latex. Each immersion in the latex was followed by a drying step at a temperature sufficient to drive off the water, ca. 95–110°C [11]. Each pass resulted in a coating thickness of ca. 0.03 mm, and multiple passes were used to obtain a final thickness of ca. 0.13 mm.

Following casting, the film could be cured by heating it to promote the cross-linking of the elastomeric component. The curative used in these samples was N,N′-dicinnamylidene-1,6-hexane diamine (Diak #3, DuPont) which undergoes hydrolysis to form cinnamaldehyde and hexamethylene diamine. Above 100°C, the hexamethylene diamine reacts to form covalent cross-links in fluoroelastomers which incorporate vinylidene fluoride in their composition [12,13]. This curing step was performed by first layering uncured or *greenleaf* plies of the material until a desired thickness (typically 0.64–1.02 mm) was reached. Care was taken in stacking the films to minimize the formation of voids between the layers. Under pressure, the tackiness of the greenleaf film compounded the plies into a uniform sheet. Sections of the material were cut to fit the two presses (from F.S. Carver, Inc.) used for curing: a Model M press ($22.9 \times 22.9\ cm^2$) and a Model CMV50H-13-C press ($45.7 \times 45.7\ cm^2$). The curing step for these materials was performed by holding the films at 300 psi for 30 min at 177°C. An additional post-curing step was used for some samples, which involved holding the films under atmospheric pressure for 20 h at 204°C.

Prior to casting, the formulation components of Table 1 were blended together according to the following procedure. First, the curative agent (DIAK #3, Dupont) and the surfactants (non-ionic surfactant Daxad 11, Hampshire Chemical and ionic surfactant ammonium caseinate in a

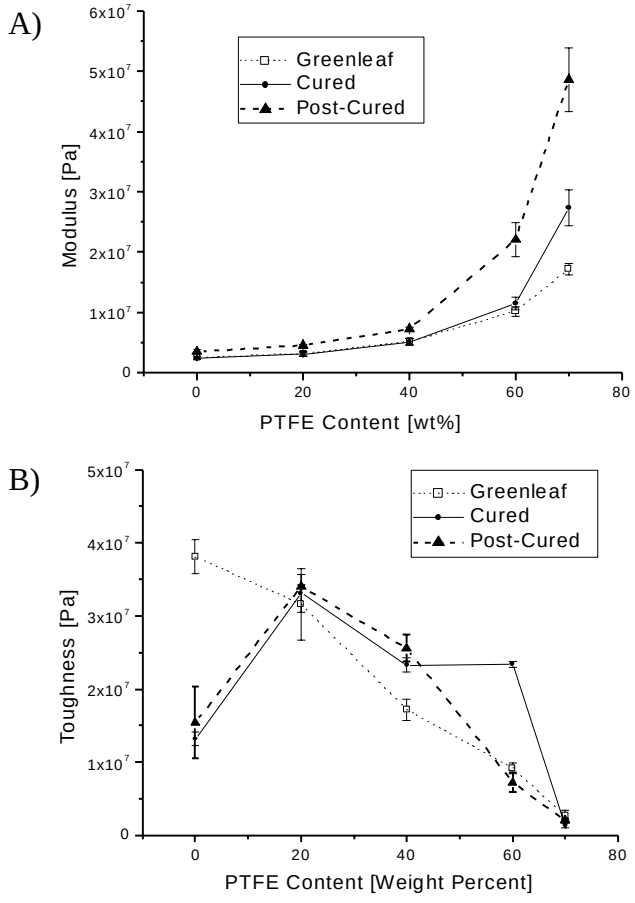

Fig. 1. Summary of data from Instron tensile tests at room temperature: (A) Young's modulus and (B) toughness.

10% dispersion, Technical Industries) were ball milled until well mixed and then de-aerated. As stated earlier, the fluoroelastomer used in this study is a terpolymer of tetrafluoroethylene, vinylidene fluoride, and hexafluoropropylene; and it will be referred to as 'FKM'. The FKM used for most of this study will be referred to as 'FKM A'. Unpublished work by another laboratory at Virginia Tech determined that this FKM has a mole percent ratio of 14.9/65.2/19.9 TFE/VF_2/HFP [14]. Aqueous zinc oxide (60% solids, Technical Industries, Inc.) was mixed into the concentrated FKM latex followed by the Diak mixture. Finally, the high molecular weight PTFE dispersion (ca. 60 wt% solids) was stirred in gently to minimize shear. Following the addition of these components, the blend was de-aerated for 1 h under a vacuum of 20 in. of mercury, whereupon it was then ready to be cast on to the carrier substrate as described in Ref. [11].

The level of PTFE was varied to produce samples at 0, 20, 40, 60, and 70 wt% PTFE relative to the FKM, while keeping the ratio of all of the other components to the FKM constant. For each level of PTFE content, greenleaf (i.e. not cured), cured, and post-cured samples were produced. As stated earlier, the intensity average particle size for the PTFE dispersions was found via light scattering to be 0.2 μm.

2.2. Methods

Dynamic mechanical analysis (DMA) was performed on a Seiko Model 210 in the tensile mode. The samples were heated from −110 to 400°C at a rate of 2°C/min, and the storage modulus (E') and tan δ data were collected at a frequency of 1 Hz. Bar shaped samples were cut from the films and had dimensions of approximately $0.1 \times 5 \times 15$ mm^3 with a grip-to-grip distance of 10 mm.

The mechanical properties were also investigated at room temperature (ca. 22°C) through tensile testing based on ASTM D412 using an Instron 4400R equipped with a 1000 N load cell and Instron Series IX controller software. Dogbone shaped samples were cut having gauge sections 6.5 mm long by 2.8 mm wide. Thicknesses were typically ca. 0.15 mm. A 10 mm grip-to-grip distance was used and the crosshead speed was 200 mm/min. To evaluate the thermal dependence of mechanical properties, some tests were also performed in an environmental chamber produced by Russells Technical Products using a Watlow 922 microprocessor for environmental control. Samples were allowed to condition for 15 min at the test temperature, and humidity was not controlled. Tests were performed over the range from 5 to 55°C. Samples used in the thermal dependence part of this study contained no curative, precluding the formation of any cross-links. Typical greenleaf materials do contain curative and are known to form some covalent cross-links due to heating in the drying step of the sample preparation.

The variation of the degree of covalent cross-linking between the greenleaf, cured, and post-cured samples was evaluated via solvent extraction using 2-butanone (methyl ethyl ketone). Elastomeric samples (0 wt% PTFE) were held in boiling solvent, and the solvent was drained and replaced six times at 8 h intervals. After removal from the solvent, all samples were dried at 100°C at 30 in. of mercury vacuum.

The morphology of the solid state films was principally investigated using transmission electron microscopy (TEM). From samples embedded in epoxy at 60°C, very thin sections were cryogenically microtomed using a diamond knife on a Reichert–Jung Ultracut-E ultramicrotome, with the FC-4D cryo-attachment operating at −90°C. Ethanol was used to collect the sections on to 600 mesh copper grids. Micrographs were taken using a Philips Model 420 T scanning transmission electron microscope (STEM) operating at an accelerating voltage of 100 kV. At least three magnifications were taken for each sample. 'High' magnification refers to 37,500× on the negative, 'medium' refers to 10,500× on the negative, and 'low' refers to 3300× on the negative.

Atomic force microscopy (AFM) in tapping mode was

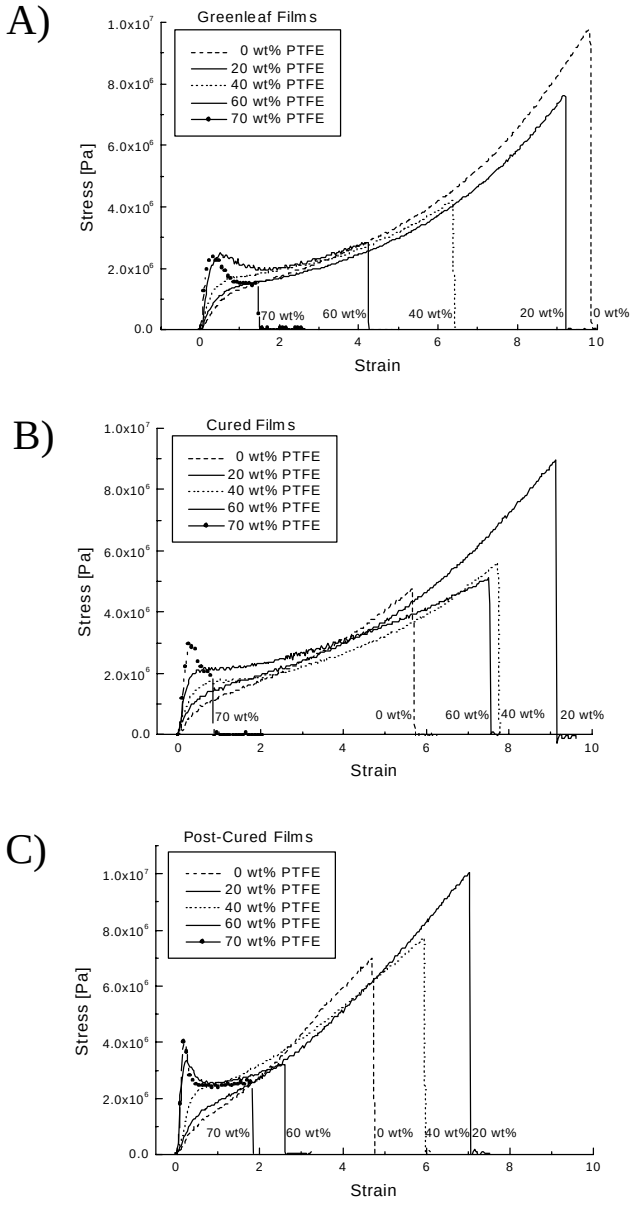

Fig. 2. Room temperature stress–strain behavior comparing different levels of PTFE content for materials that are: (A) greenleaf; (B) cured; and (C) post-cured.

also used to study the nanoscopic level structure. Experiments were performed on a Digital Instruments scanning probe microscope using nanosensors tapping etched silicon probe (TESP) type single beam cantilevers. These cantilevers had nominal lengths of ca. 125 μm, force constants of approximately 35 ± 7 N/m, and were used at oscillation frequencies of ca. 290 kHz. All the AFM micrographs presented here are phase images of the film surfaces. However, cross-sections of films could be imaged via AFM micrographs by examining the surfaces of samples mounted in epoxy for TEM after being smoothed by cryomicrotoming.

3. Results and discussion

3.1. Mechanical and viscoelastic properties — tensile tests

The dependence of the mechanical and viscoelastic properties of these materials on the level of PTFE content and covalent cross-linking were investigated through tensile elongation testing and DMA. The modulus data presented in Fig. 1(A) suggests that the difference between the greenleaf and the cured materials is only detectable at a higher PTFE content, but that post-curing provides enough cross-linking to increase the modulus significantly. For example, whereas the cured materials could only be distinguished from the greenleaf films above 50 wt% PTFE content, the post-curing increased the modulus at all PTFE levels by an average of ca. 120% over the modulus of the uncured samples. Fig. 1(A) also suggests a dramatic increase in the modulus above 50 wt% PTFE, which may indicate some development of connectivity between the PTFE filler particles. While some increase is observed as the PTFE content is increased from 0 to 40 wt%, it is a minor change in comparison to the modulus increase provided by the cross-linking. For example, the 20 wt% PTFE film after post-curing exhibited the same modulus as the 40 wt% PTFE greenleaf or cured films. On the other hand, as PTFE begins to form the majority of the matrix, the level of PTFE content can be seen to become more important to the final modulus of the film. Specifically, the modulus of the 60 wt% green leaf or cured films is higher than that of the post-cured 40 wt% film, indicating a greater increase based on the PTFE level. Fig. 1(A) also shows that the increase in modulus due to cross-linking is multiplied by increasing the level of PTFE content particularly above 50 wt%.

In tensile testing, the 'toughness' is calculated by numerically integrating the stress–strain curve and this provides a measure of the energy per unit volume absorbed by the material before it breaks. As Fig. 1(B) shows, the toughness of the films varies significantly relative to the PTFE content and the degree of cure. Prior to curing, it can be seen that the toughness systematically decreases with PTFE content from 38 MPa at 0.0 wt% PTFE to 3 MPa at 70 wt% PTTE. The convolution of the PTFE content with the degree of cure alters the behavior significantly. For example, the toughness of the cured and post-cured materials is ca. 14 MPa at 0 wt% PTFE and it increases to ca. 33 MPa at 20 wt% before decreasing back to 2 MPa at 70 wt%. This behavior is not unexpected in view of the uncross-linked weaker matrix phase whose failure is enhanced by the stress concentrator effect promoted by the more rigid filler PTFE phase. As compared to the greenleaf materials in the range of 20–60 wt%, curing or post-curing the films appears to reduce the rate of toughness loss as the PTFE content is increased. To understand this behavior, a closer examination of the stress–strain curves is required.

Fig. 2(A) shows the representative stress–strain behavior

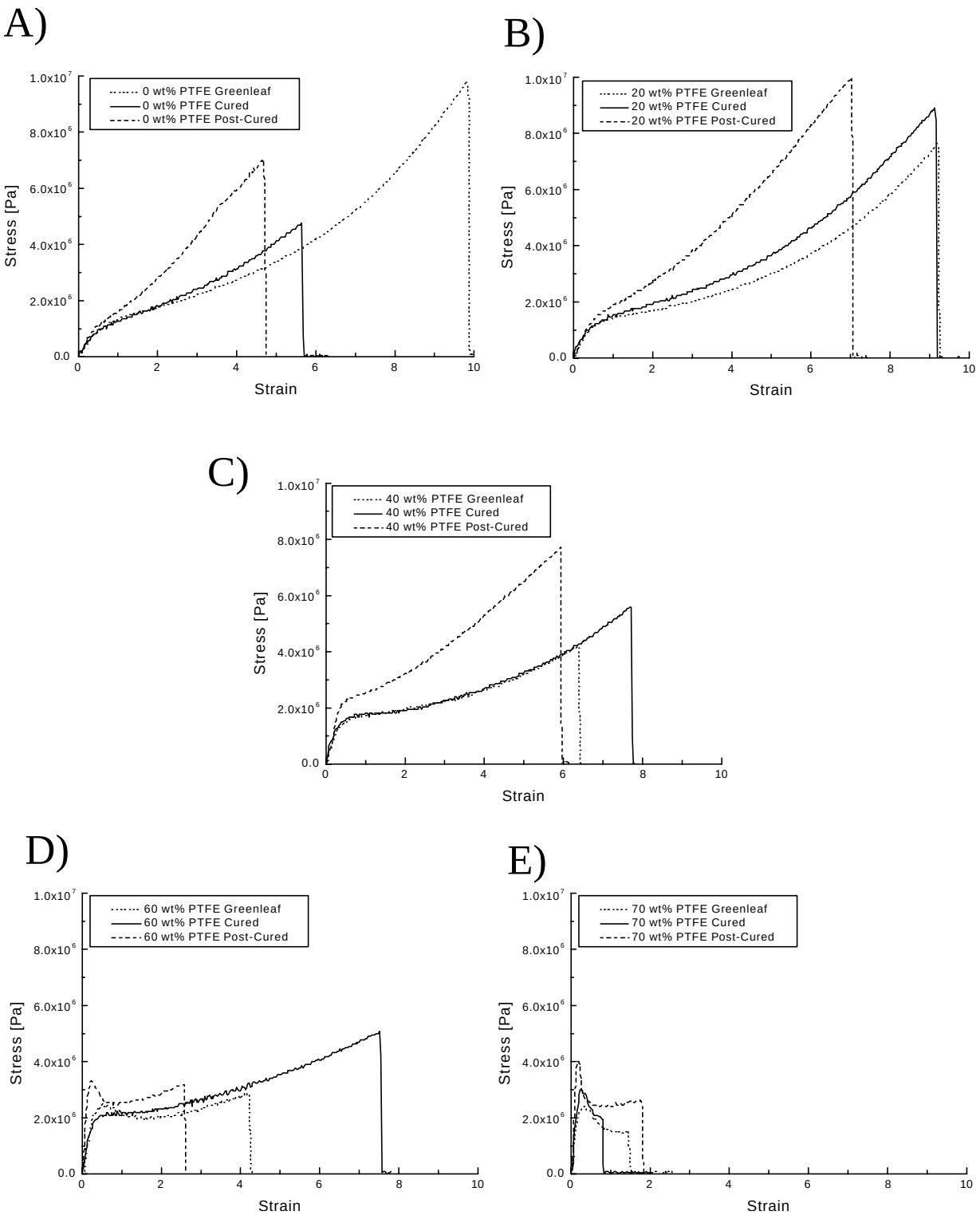

Fig. 3. Room temperature stress–strain behavior comparing the degree of cross-linking at each level of PTFE content: (A) 0 wt%; (B) 20 wt%; (C) 40 wt%; (D) 60 wt%; and (E) 70 wt%.

of the greenleaf materials, revealing two systematic trends: the modulus increases and the strain-at-break decreases with increasing PTFE content. It is also interesting to note that the character of the curves shifts from being very typical of elastomeric deformation behavior at 0 wt% PTFE to having a more plastic character at 70 wt% PTFE. This can be seen in that as the PTFE fraction is increased, a yield point develops and becomes much more distinct; also, the draw region

or the irrecoverable flow region becomes easier to distinguish. Similar alterations in the character of the stress response have been observed in elastomeric systems that have been reinforced with inorganic fillers such as rock salt and glass beads [15]. This behavior is considered to result from the close packing which occurs at higher filler contents. In other words, as the composite material is stretched, the close proximity of the filler particulate not only promotes stress concentration but may also impede local large scale deformation from occurring, which results in much lower strain-at-break values.

The cured and post-cured materials exhibit behavior that is less straightforward. As the representative curves in Fig. 2(B) and (C) show, the moduli of the materials systematically increase with the PTFE content. Also, like in the greenleaf films, the yield point and draw regions become more distinct. Unlike the greenleaf materials, however, the strain-at-break behavior is significantly different. For the cured materials, the strain-at-break is relatively constant with respect to the PTFE content remaining in the 8–9 strain units region between 20–60 wt% PTFE. This is two strain units higher than the point of break for the 0 wt% PTFE film. Likewise, the post-cured materials with 20 and 40 wt% PTFE exhibit an increase in the strain-at-break over the 0 wt% PTFE post-cured sample. This is important to note because, after the initial yielding behavior (ca. 0.5 strain), the stress–strain curves of Fig. 2(B) are remarkably similar regardless of the PTFE content. Fig. 2(C) displays similar stress–strain behavior.

This mechanism appears to depend upon the interaction of the cross-linking with the level of PTFE content. Examining the variation of the degree of cure at each level of PTFE content separately can facilitate discerning the nature of that mechanism. Fig. 3(A) reveals that with no PTFE particulate present, the strain-at-break decreases systematically from 10 in. the greenleaf film to 4.8 in. the post-cured sample. Even with the lowest PTFE fraction studied, Fig. 3(B) suggests that adding 20 wt% PTFE significantly alters the mechanical behavior. Both the uncured and the cured films broke at the same strain (ca. 9.2) and the cured sample exhibited higher load bearing, breaking at a stress of 8.8 MPa compared to 7.5 MPa for the uncured film. The post-cured sample also exhibited higher load bearing at each strain, which must be a result of the higher level of cross-linking. Similar behavior of increasing load bearing capability with increasing level of cross-linking can also be observed in the 40 wt% PTFE material in Fig. 3(C). In summary, Fig. 3(A) shows that without the PTFE particles, cross-linking results in breaking at lower strain levels; however, Fig. 3(B) and (C) indicates that adding PTFE particulate increases the toughness by maintaining or increasing the strain-at-break while raising the load bearing.

The stress–strain behavior of the 20 and 40 wt% PTFE cured and post-cured films demonstrates further that the draw or irrecoverable flow domain of the response curve, in addition to the increase in load bearing, is responsible for the increases in toughness as the material is cross-linked. These data suggest two conclusions regarding the interaction of the PTFE content with the level of cross-linking. First, they indicate that in the presence of cross-linking enough stress is transferred to the PTFE particles to improve the toughness. This could occur either by distributing the stress more evenly throughout the material and/or by the PTFE undergoing a relaxation mechanism of its own. The other conclusion suggested by the stress–strain data is that without cross-linking, enough strain is not borne by the PTFE component to increase the toughness. In other words, it is hypothesized that without cross-linking, the stiffness of the elastomer at room temperature is too low to transfer enough stress to the PTFE particles to increase the toughness.

This hypothesis can be tested by examining the thermal dependence of the stress–strain behavior of specially fabricated greenleaf films. Typical greenleaf films (i.e. those studied in most of this work) do contain curative agents but do not see a curing step following casting. Some level of cross-linking is generally thought to occur during the drying step, however, as will be discussed in Section 4. For this part of the study, three films were therefore made that contained no curative, thus allowing for the thermal influences to be tested without any potential for cross-linking. As can be seen in the 0 wt% PTFE in Fig. 4(A), the 40 wt% PTFE in Fig. 4(B), and in the 60 wt% material in Fig. 4(C), there is a strong influence of temperature on the response to deformation in the thermal range from 0–20°C. Because the glass transition of the FKM component occurs at ca. −10°C at 1 Hz in DMA testing, the viscosity of the FKM is understood to be changing rapidly in that range. At 5°C and at the rate of deformation used, the materials behave as ductile plastics, exhibiting distinct yield points and undergoing irrecoverable flow. As the temperature approaches 19°C, the materials are so extensible that the Instron could not extend far enough to stretch them to the breaking point. It is hypothesized that the high extensibility at these temperatures is augmented by the fact that the nascent crystalline PTFE must have very few entanglements as suggested earlier. Above 19°C, the FKM viscosity drops so much that the rapid stress relaxation in the films leads to loss of load bearing capability at systematically lower strain values.

The moduli data from these tests are summarized in Fig. 5(A). These data again show the increase in modulus with the increased PTFE content of the film, and the clear increase in modulus as the temperature approaches the glass transition of the elastomeric matrix. As the temperature is decreased, it also appears that the 60 wt% PTFE material undergoes a step jump in modulus at ca. 19°C and it is hypothesized that this occurs as a result of the PTFE crystal–crystal transition which occurs at that temperature which influences the deformability of the PTFE particles. The toughness data from these experiments is exhibited in

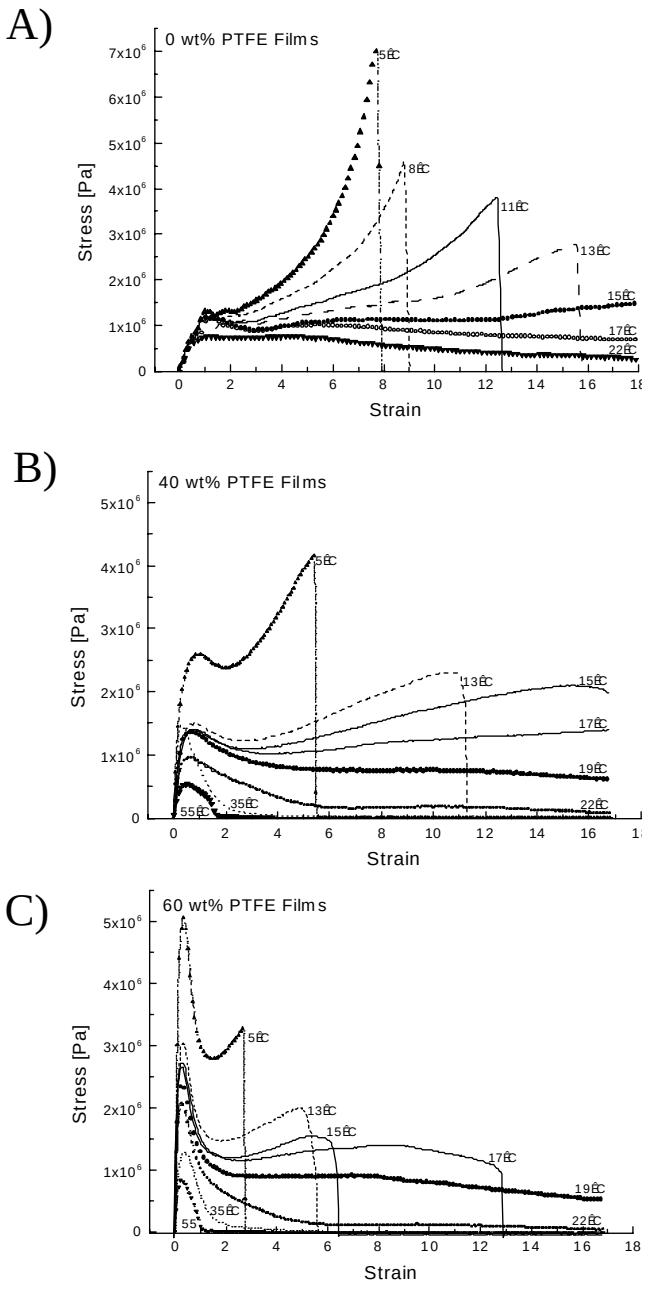

Fig. 4. Thermal variation of the stress–strain behavior for the greenleaf materials. Stress–strain curves for: (A) 0 wt% PTFE; (B) 40 wt% PTFE; and (C) 60 wt% PTFE.

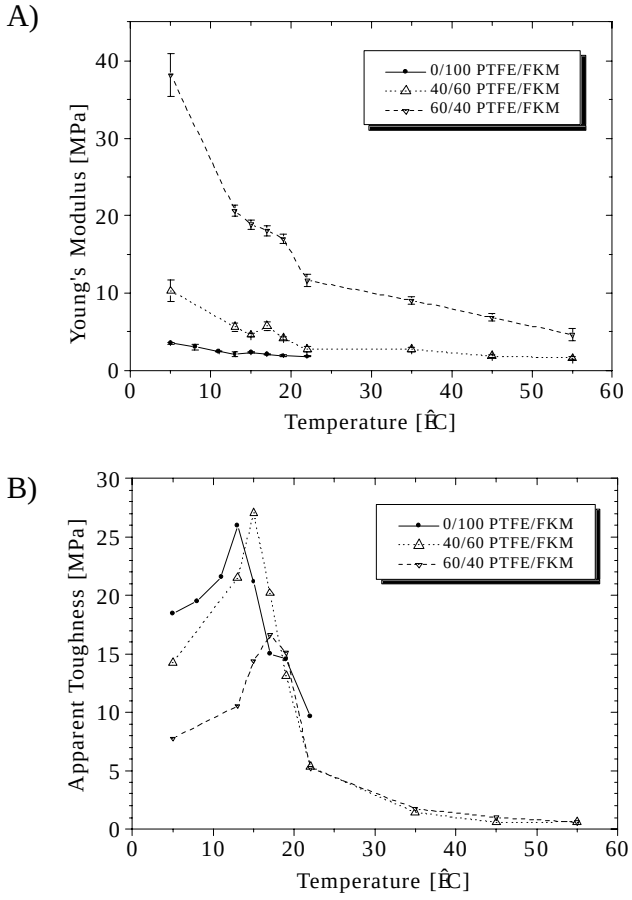

Fig. 5. Summary of the thermal variation tensile tests: (A) modulus and (B) toughness.

Fig. 5(B) which shows, as Fig. 4(A)–(C) suggested, that the materials have the greatest toughness in the thermal range of 13–19°C. The strong maximum in Fig. 5(B) at 15°C for the 40 wt% PTFE films should be recognized to be lower than the true peak as a result of the 17 and 19°C materials not breaking in the Instron. The 60 wt% material indicates that the true peak in toughness occurs at ca. 19°C. Although the toughness peak for the 0 wt% film was incompletely determined because fewer of its samples broke in the test instrument, it is possible that the peak in toughness observed at 19°C for the 60 wt% sample was due to the presence of the PTFE particulate and not to the elastomer alone. Therefore, this toughness peak behavior is suggested to result from increasing the transfer of shearing forces from the elastomeric matrix to the PTFE particulate. Furthermore, it is hypothesized that as the viscosity of the elastomer is modified either by cross-linking or by thermal variation, more of the load is transferred to the PTFE component resulting in increased toughness.

Although not a key part of this study, it was of interest to compare the modulus data for the greenleaf systems to the standard theories of filled system behavior. Three approximations were applied: the Guth–Smallwood equation Eq. (1), the Kerner equation Eq. (2), and the Mooney equation Eq. (3) [16–18].

$$E = E_1[1 + k_E\phi_2 + 14.1\phi_2^2] \tag{1}$$

$$E = E_1\left[1 + \frac{\phi_2}{\phi_1}\left(\frac{15(1-\nu_1)}{8-10\nu_1}\right)\right] \tag{2}$$

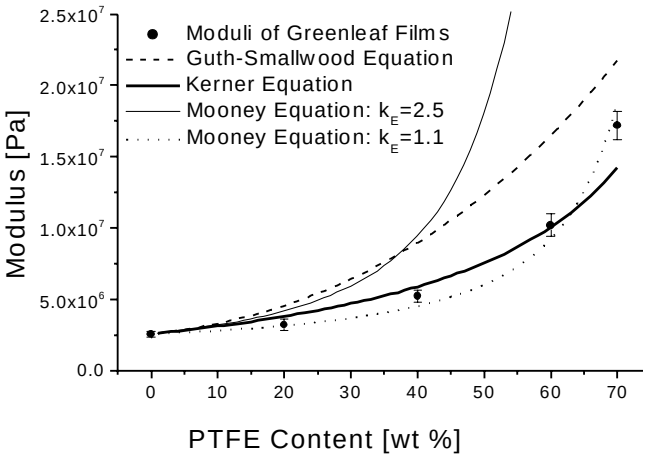

Fig. 6. Comparison of the experimental data with various theories of filled materials.

$$E = E_1 \exp\left[\frac{k_E \phi_2}{1 - (\phi_2/\phi_M)}\right], \quad (3)$$

where E is the observed modulus of the filled system; E_1 the modulus of the matrix; k_E Einstein's coefficient, 2.5 for well-dispersed, wetted spherical filler; ϕ_1 and ϕ_2 the volume fractions of matrix and filler, respectively; ν_1 Poisson's ratio of the matrix; and ϕ_M the maximum filler volume fraction (1.0 is maximum, 0.714 fits most data).

As shown in Fig. 6, the Kerner and the Mooney equations provided the best predictions for the action of the reinforcing PTFE. The quality of the fit of the Kerner equation suggests that its assumptions as applied here may be reasonable. These assumptions are that Poisson's ratio of the matrix is 0.5 and that the PTFE particulate is much more rigid than the matrix. The Guth–Smallwood and the standard (i.e. $k_E = 2.5$) Mooney equations showed reasonable agreement below 20 wt%, as observed in many other systems [16,18], but both over-predicted the moduli above this PTFE content. This was expected based on their derivations for systems with low filler volume fractions [16,18]. It was found that the Mooney equation is not strongly dependent upon the value of ϕ_M used, but that it does vary significantly with k_E. As stated earlier, the coefficient k_E in the Mooney equation is equal to 2.5 for well-dispersed spherical particles; however, as shown in Fig. 6, when this is adjusted to 1.1, the equation fits very well. Since the assumption that $k_E = 2.5$ is not valid, this may suggest that the PTFE is not functioning as a well-dispersed, 'wetted' spherical filler in the FKM matrix. Because little interpenetration of the FKM and PTFE phases is expected, due to the high crystallinity of the PTFE phase, an alternative hypothesis is that the PTFE does not have good adhesion to the matrix. Thus, voids may be developing as the film is deformed or the matrix may be flowing around the PTFE particles.

3.2. Mechanical and viscoelastic properties — dynamic mechanical analysis

To further examine the thermal dependence of mechanical properties, these materials were tested using DMA. In Fig. 7(A), (C) and (E), the storage moduli of the greenleaf, cured and post-cured materials are compared at various levels of PTFE content. Only minimal differences could be observed in the glassy state (below −25°C), although the higher PTFE content films tended to exhibit slightly higher storage moduli. It can also be seen in Fig. 7(A), (C) and (E) that the relaxation rate near the glass transition (ca. −10°C) systematically decreases for each higher level of PTFE content. However, no corresponding variation in the location of the tan δ peak was observed, as shown in Fig. 7(B). These two observations suggest that the phases are relatively well separated (i.e. the FKM tan δ peak does not shift) and that PTFE is adding a new relaxation slightly above the FKM glass transition. This hypothesis will be elaborated on below. As observed with the tensile testing, the storage moduli systematically increase with each higher level of PTFE content above the FKM glass transition at ca. −10°C.

Fig. 7(B) also shows more clearly than Fig. 7(A) that the glass transition region steadily becomes broader as PTFE particulate is added. This suggests that adding the filler widens the range of molecular mobilities in the blended material. These figures clearly reveal, however, that the ca. −10°C peak of the FKM glass transition does not shift to higher temperatures, but rather only the high temperature side of the tan δ peak base appears to broaden. In the light of the dramatic change in the magnitude of the tan δ peak but a lack of any change in its location, this skewed basal broadening is hypothesized to indicate a separate, higher temperature relaxation mechanism not related to the FKM phase. As PTFE is added, the peak is systematically reduced from 1.4 at 0 wt% PTFE to 0.4 at 70 wt% PTFE. This expected behavior correlates well with the reduction in material in the film that is undergoing its glass transition at that temperature.

The cured and post-cured materials show many similar trends observed in the greenleaf films. The storage moduli are presented in Fig. 7(C) and (E), and the respective tan δ curves are presented in Fig. 7(D) and (F). One difference between these and the greenleaf films is the narrowness of the FKM glass transition in the 0 wt% PTFE cured and post-cured materials observed in Fig. 7(C) and (E). It can be observed there that the flat rubbery plateau is reached at ca. 0°C, instead of 150°C as in the greenleaf film. It is hypothesized that the greenleaf materials would have a similar distinctness to their glass transitions if they could be adequately dried after casting without cross-linking. Since water is a by-product of the cross-linking reactions, an alternate hypothesis is that water is evolving in the greenleaf films as they are heated during the DMA test. Similar to the greenleaf films, Fig. 7(C) and (E) shows that

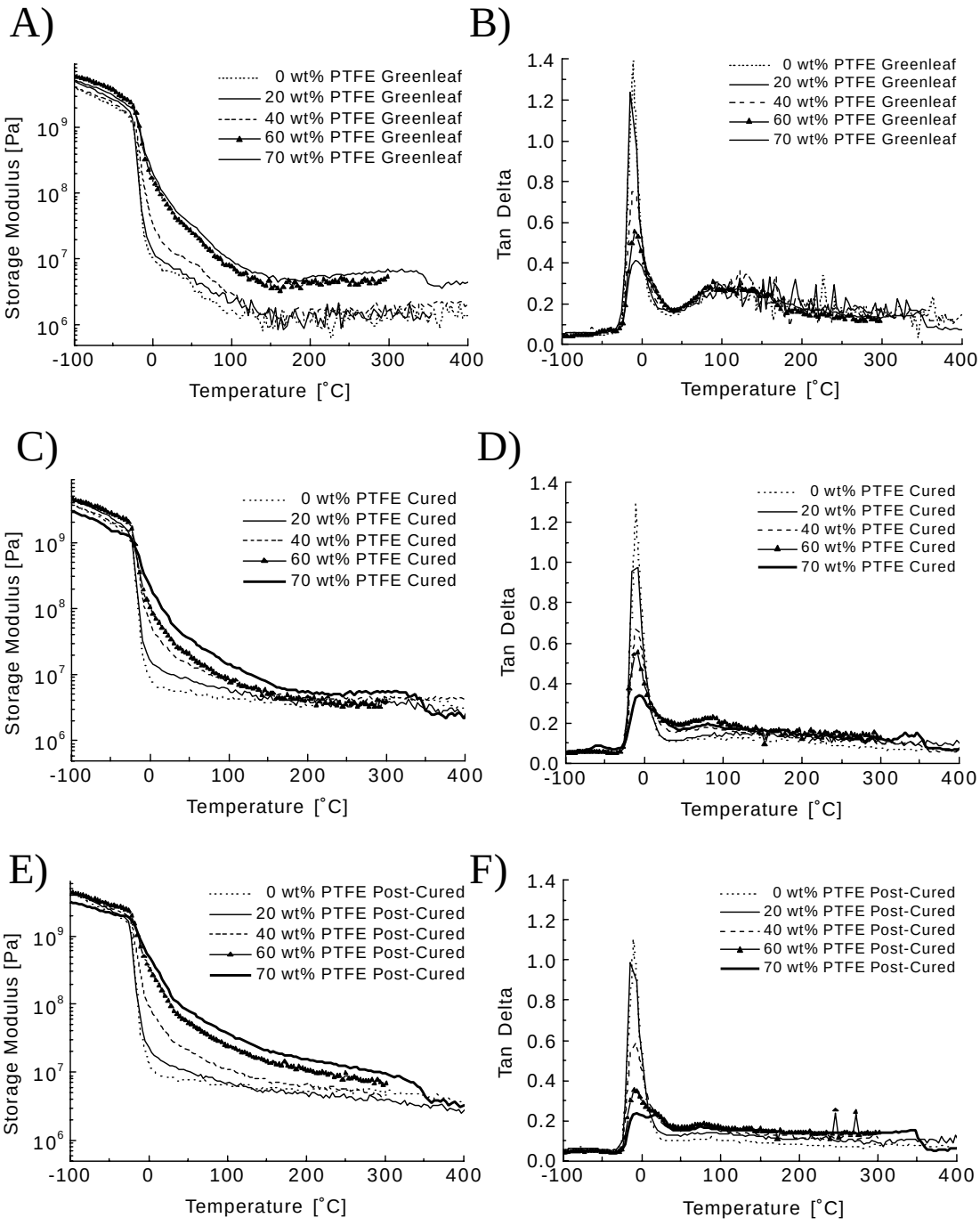

Fig. 7. Influence of PTFE wt% on the DMA results: (A) storage moduli and (B) tan δ curves of greenleaf materials; (C) storage moduli and (D) tan δ curves of cured materials; and (E) storage moduli and (F) tan δ curves of post-cured materials.

increasing the PTFE content systematically increases the storage moduli in the rubbery region. In terms of altering the character of the thermal spectrum of the storage modulus, however, the most significant effect of adding the PTFE is the broadening of the glass transition region at ca. −10°C. As will be shown in the tan δ analysis of Fig. 8, this broadening is considered to result from the convolution of the FKM glass transition at ca. −10°C with the PTFE crystalline transitions. The glass transition in Fig. 7(C) and (E) is observed to become consistently more indistinct as the PTFE component is increased, until a truly flat rubbery plateau cannot even be identified in the 60 and 70 wt% PTFE post-cured films as compared to the 0 wt% PTFE films. Also, in comparing Fig. 7(C) and (E), it may be observed that in the range of 200–350°C the level of PTFE content only increases the storage modulus

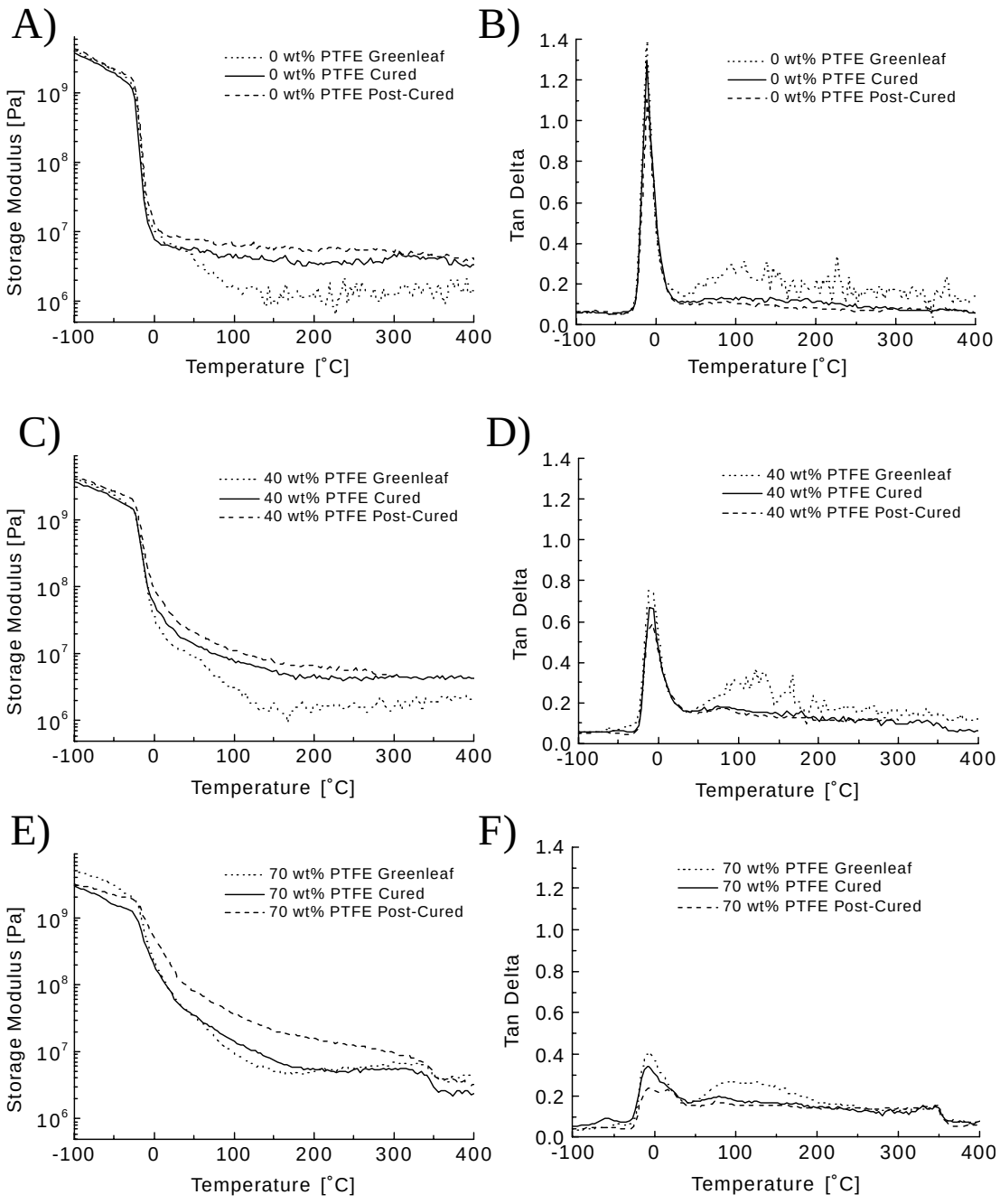

Fig. 8. Influence of cross-linking on the DMA results: (A) storage moduli and (B) tan δ curves of 0 wt% PTFE films; (C) storage moduli and (D) tan δ curves of 40 wt% PTFE films; and (E) storage moduli and (F) tan δ curves of 70 wt% PTFE films.

in the post-cured materials. Finally, it can be noticed in all the storage moduli data that as the PTFE fraction of the composition is increased, a distinct relaxation occurs at ca. 350°C and this corresponds to the melt temperature of the PTFE.

An interesting observation is that a minor peak appears in the tan δ curves of the 60 and 70 wt% PTFE films at ca. 80°C. It is especially clear in the post-cured films of Fig. 7(F) that this peak only occurs at high PTFE content, suggesting that, just as with the PTFE melting peak at 350°C, this relaxation is occurring only in the PTFE phase of the film. This is corroborated by studies on pure PTFE which have shown that a beta relaxation peak occurs at ca. 100°C for highly crystalline PTFE materials [19].

To display more clearly the effects of PTFE content on the influence of cross-linking on DMA behavior, some of the data from Fig. 7 are replotted in Fig. 8. Fig. 8(A) and (B) represents the 0 wt% PTFE films, Fig. 8(C) and (D) the

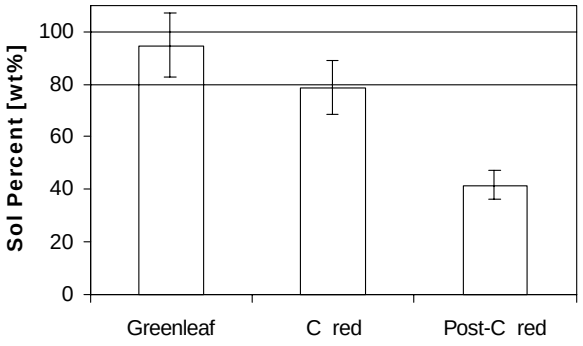

Fig. 9. Degree of covalent cross-linking characterized by solvent extraction where sol percent represents the weight percent of extractable material.

40 wt% PTFE films, and Fig. 8(E) and (F) the 70 wt% PTFE films. The data for the 20 and 60 wt% films are not presented because they exhibited the same trends shown by the other blend compositions. It can be clearly observed in the storage modulus graphs of Fig. 8 that all the greenleaf films exhibit a distinct shoulder beginning at ca. 25–50°C which, as discussed earlier, correlates well with the broad transition observed in the tan δ plots at ca. 50–150°C. This shoulder is conjectured to originate potentially in the vaporization of water which either remains from casting the film or is evolved during curing of the FKM phase as the DMA test proceeds. It may also be observed on comparing the tan δ plots of Fig. 8, that the basal broadening of the main peak only occurs as PTFE is added. In Fig. 8(B), the peak appears very sharp, ending at ca. 10°C for all levels of cure. In Fig. 8(D), the peak appears to be skewed so that it ends in the ca. 20°C range. Finally, in Fig. 8(F), it is clear that a second transition is underlying the main FKM transition and is causing the apparent skew. Since this peak appears to become more pronounced at higher PTFE contents and since a PTFE crystalline transition is known to occur at ca. 19°C, it is hypothesized that this second peak is solely related to the PTFE phase.

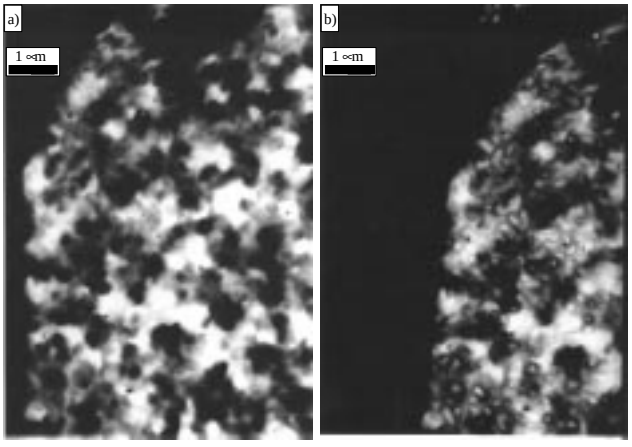

Fig. 10. TEM micrographs: (a) showing the development of electron beam damage in an as-cast greenleaf film containing 60 wt% PTFE and (b) showing the same area following the onset of radiation damage.

4. Polymer morphology

Characterization of the solid state was performed with solvent extraction, AFM, and TEM. Solvent extraction was performed to characterize the formation of covalent cross-links during the curing and post-curing steps in the 0 wt% PTFE samples. The samples were kept in boiling solvent until the greenleaf materials were solubilized as much as possible; however, none of the greenleaf films tested were completely soluble. As shown in the data of Fig. 9, ca. 95% of the greenleaf material was extractable, indicating that an extensive three dimensional covalent network has not formed due to heating in the drying steps of the film production. It was not completely soluble, however, suggesting that some degree of cross-linking has occurred. After curing, ca. 79% of the films were extractable. This is a relatively small change and it suggests that little of the material is bound into a covalent network. The post-curing steps resulted in substantially more cross-linking as only ca. 42% of the material was extractable. These latter data illustrate that even with the conventional cross-linking methodology utilized, a significant sol fraction still existed which indicates the difficulty in promoting a fully cross-linked network in fluoroelastomers produced by these methods. These results also correspond well with the mechanical behavior, in that little change occurs as a result of the curing step but that the post-cure induces significant levels of cross-linking.

TEM provides a 2-D projection of a ca. 70–110 nm thick cross-section of the film. Using TEM to characterize these materials presented one large difficulty in that the PTFE particulate rapidly undergoes chemical changes upon exposure to the electron beam. Upon initial viewing the 0.2–0.5μm PTFE particulate appears darker than the elastomer indicating higher electron density than the matrix, which is expected given the high crystallinity of the PTFE. Within 5–15 seconds, however, the particulate in the matrix turns white indicating strong interaction with the electron beam. It is hypothesized that this change may be due to chain scission and degradation caused by the electron beam, as has been noted in PTFE by other workers [20,21]. The beam damage occurred too quickly to collect micrographs at higher (at or above ca. 10,500 ×) magnification. However, by focusing on one place and then moving to an adjacent area and then collecting the image immediately, it was possible to observe the morphology at ca. 3,300 × before it changed. Magnifying from the negative provides the close views shown in Fig. 10. Fig. 10(a) is the micrograph collected initially, and it may be seen that the black PTFE particles have a much higher electron density than the white FKM matrix. Also it may be noted that, prior to the onset of beam damage, the particles appear to be aggregated and to

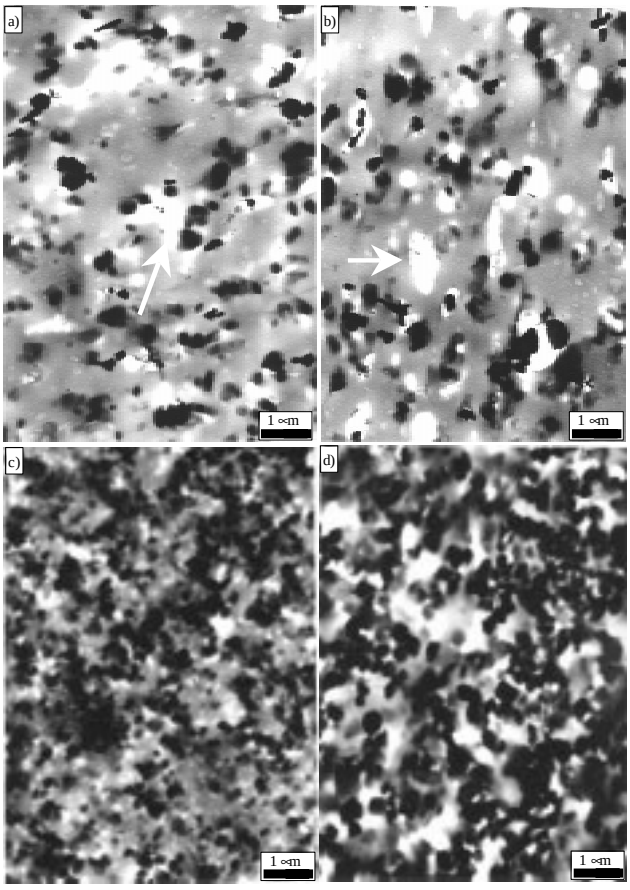

Fig. 11. TEM micrographs of as-cast greenleaf films containing (a) and (b) 20 wt% PTFE, (c) 40 wt% PTFE, and (d) 60 wt% PTFE. White arrows indicate 'pull-out' artifacts.

exhibit some apparent connectivity. This correlates well with the stress–strain behaviour of Fig. 2. Fig. 10(b) was collected ca. 15 seconds later, and it may be seen that the beam damage has significantly altered the morphology. The FKM appears darker, and the PTFE particles appear smaller and whiter. This indicates that the PTFE has lost electron density. Also, even in this incompletely damaged sample the particles appear less aggregated and interconnected. These changes suggest that detecting alteration in polymer morphology requires collection and analysis of micrographs of the cross-sections prior to the onset of beam damage.

The four micrographs of Fig. 11 examine the morphology of as-cast films as a function of PTFE content. Fig. 11(a) and (b) shows that at 20 wt% PTFE, the films show some ca. 1–2 μm clusters of discrete particles that are separated by ca. 1 μm of relatively PTFE poor regions. Also, Fig. 11(a) and (b) presents the first micrographs in which particle 'pull-out' may be observed, as indicated by the arrows. This is an artifact which occurs when the knife comes to a particle much thicker than the ca. 70–100 nm thick section it is cutting. Rather than cut, the particle merely pulls out of the section leaving a hole. This frequently occurs in composite materials where there is no significant bonding/adhesion between the matrix and the filler.

Fig. 11(c) and (d) shows the morphology of films with 40 and 60 wt% PTFE, respectively. It should be noted that the section is somewhat thicker in Fig. 11(c) resulting in the appearance of more PTFE particles. The tendency of the PTFE particles to form clusters may be observed in all the micrographs. The difference between the samples appears to be the frequency of the PTFE poor domains. As the weight

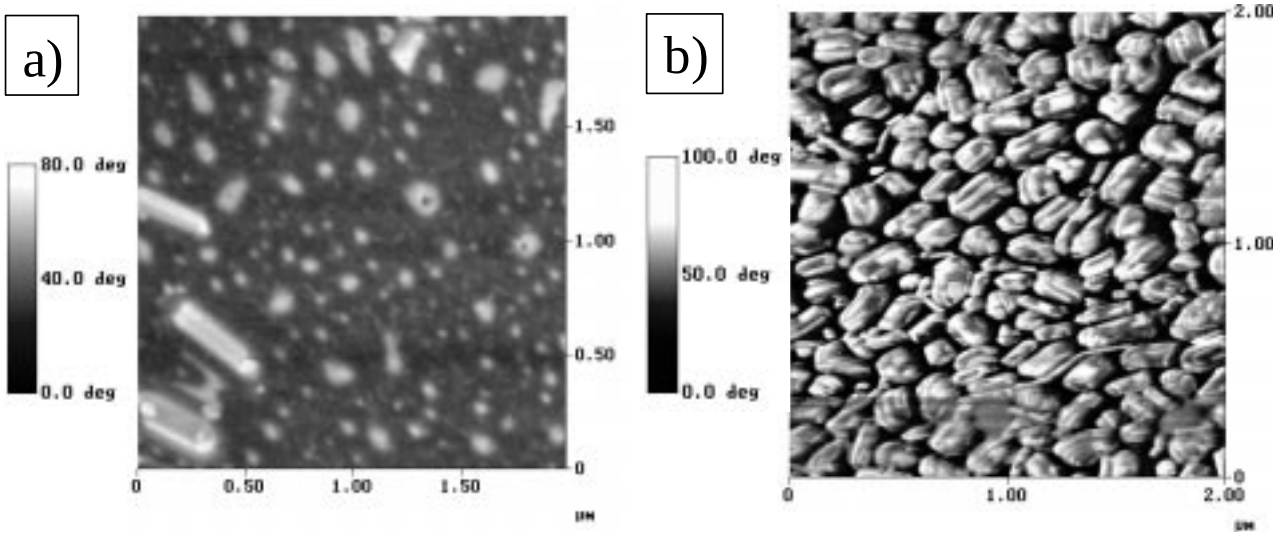

Fig. 12. Phase images from tapping-mode AFM: (a) of the carrier film side of a 20 wt% PTFE film and (b) of the carrier side of an 80 wt% PTFE film.

percent of PTFE is increased, space filling considerations reduce the distance between the PTFE particle clusters. Thus, the 60 wt% PTFE film of Fig. 11(d) exhibits the most even distribution of PTFE particles.

When compared to the experimental challenges of TEM, tapping-mode AFM is a technique that is ideal for studying the surface-plane morphology of thin films. Phase imaging with AFM is based on tracking phase offsets or differences between the drive oscillation to the cantilever probe and the actual oscillation of the cantilever tip as it interacts with the surface of the sample. For the instrument used at typical drive amplitudes, harder material induces higher phase offsets which are shown as white in the phase images. Thus, as shown in Fig. 12(a), PTFE particulate are shown as white corresponding to high phase offsets and the elastomer appears as a moderate phase offset. In the non-deformed samples, these micrographs showed great similarity to the results from TEM. As can be seen in Fig. 12(a), at 20 wt% PTFE, particulate are seen to be dispersed in the FKM matrix. Unlike the TEM micrographs, Fig. 12(a) does not reveal structure larger than ca. 0.3 μm. However, because AFM only reveals structure to a depth of ca. 10 nm, it is not expected that large particles would be fully visible unless they are oriented near to parallel with the film surface. Fig. 12(b) is a phase image of an 80 wt% PTFE film and it provides further confidence in this technique in that the same type and size of particulate are observed as in Fig. 12(a). As indicated by the arrow in Fig. 12(b), some fibril structures ca. 0.05 μm across and ca. 0.1–0.6 μm long were also occasionally observed. As this was representative of the film surface, it is unclear whether small amounts of fibrillation occur at high PTFE content during the normal casting process or whether this was induced by the handling which occurred as the film was removed from the carrier. Influences of deformation upon the structural aspects of these materials are more fully discussed elsewhere [22].

5. Conclusions

This study has elucidated the structure–property relationships of poly(tetrafluoroethylene)–poly(tetrafluoroethylene-*co*-vinylidene fluoride-*co*-hexafluoropropylene) (PTFE/FKM) cast blends. It has been shown that increasing the PTFE content of the blend or cross-linking of the FKM leads to systematically higher modulus and generally reduced toughness. In DMA, these two factors were also shown to increase the rubbery moduli of the films and to reduce the magnitude of the tan δ peak corresponding to the FKM glass transition. Temperature was also shown to have significant effects on the deformation behavior of the greenleaf (non-cross-linked) films. It was shown that, for the deformation rate utilized, there is a maximum in the toughness of the materials near 17–19°C, which is hypothesized to be a result of a maximum in the transfer of shear stress to the PTFE particles. Corresponding well with the mechanical behavior of the films, it was also demonstrated via solvent extraction that the curing step only marginally cross-links the FKM, but that the post-curing treatment leads to dramatically higher degrees of cross-linking.

TEM was used to examine the morphology of films. Some aggregation of the 0.2 μm PTFE particles was observed to occur at all levels of PTFE content studied, from 20 to 60 wt% PTFE. The main morphological difference observed to be dependent on the PTFE content appears to be the formation of micron sized domains which are relatively poor in PTFE particles. At higher PTFE contents, these domains were not observed. It is worth noting that even at 80 wt% PTFE, as studied via AFM, the FKM always forms a continuous elastomeric matrix.

Acknowledgements

The financial support of the Chemfab Corporation is gratefully acknowledged. Richard Stone is thanked for producing so many of the samples studied. Dr Baird's laboratory here at VPI&SU is acknowledged for lending us the mold used in the deformation analysis and Dr Robert Young is specifically thanked for his many insightful discussions. Finally, Steven McCartney is acknowledged for his help in the TEM examination of these materials.

References

[1] Blair JA. Fluorocarbons, polymers. Enc Ind Chem Anal 1971;13:73–93.
[2] Grot W. Tetrafluoroethylene Polymers. Enc Polym Sci Engng 1989;16:577–99.
[3] England DC, Uschold RE, Starkweather H, Pariser, R. Proceedings of the Robert A. Welch Foundation Conference on Chemical Research: XXVI Synthetic Polymers, 1983. p. 193–232.
[4] Righetti MC, Ajroldi G, Vitali M, Pezzin G. J Appl Polym Sci 1999;73:377–84.
[5] Powers J. Chem Process Mid-November 1984:145.
[6] Effenberger JA et al. US Patent Application #09/096,700. 12 June 1998, Chemfab Corp.
[7] Sperati CA, Starkweather HW Jr. Fortshr Hochpolym-Forsch: Bd. 2, S., 1961. p. 465–95.
[8] Kitamura T, Kurumada KI, Tanigaki M, Ohshima M, Kanazawa SI. Polym Engng Sci 1999;39:2256–63.
[9] Effenberger JA, Keese FM. US Pat 4,555,543. 26 November 1985.
[10] Effenberger JA, Keese FM. US Pat 5,194,335. 16 March 1993.
[11] Effenberger JA, Koerber KG, Latorra MN, Petriello JV. US Pat 4,883,716. 28 November 1989.
[12] Logothetis AL. Prog Polym Sci 1989;14:251–96.
[13] Pelosi LF. Rubber Chem Technol 1976;49:367–74.
[14] Bhattacharjee S, McGrath J.E. Presentation at ChemFab Corp, 18 July 1998.
[15] Nielsen LE. Mechanical properties of polymers and composites, vol. 2. New York: Marcel Dekker, 1974 (p. 405–8).
[16] Nielsen LE. J Compos Mater 1967;1:100–19.
[17] Nielsen LE. J Compos Mater 1968;2:120–3.
[18] Smallwood HM. J Appl Phys 1944;15:758–67.

[19] McCrum NG, Read BE, Williams G. Anelastic and dialectric effects in polymeric solids. Dover ed. New York: Wiley, 1967 (p. 452–4).

[20] Clough RL, Shalaby SW. Irradiation of polymers, fundamentals and technological applications. Washington, DC: American Chemical Society, 1996 (p. 4–256).

[21] Ribeiro CA, Vargas H, Galembeck F. J Electron Microsc 1981;30:148–9.

[22] Kaushiva BD. Structure–property relationships of flexible polyurethane foams, chap. 9. PhD dissertation. Virginia Polytechnic Institute and State University, 16 August 1999.